

Influence of Metal Oxide Nanoparticles as Antimicrobial Additives Embedded in Waterborne Coating Binders Based on Self-Crosslinking Acrylic Latex

Denisa Steinerová ^{1,*}, Andréa Kalendová ¹, Jana Machotová ¹, Petr Knotek ², Petr Humpolíček ³, Jan Vajdák ³, Stanislav Slang ⁴, Anna Krejčová ⁵, Ludvík Beneš ⁶ and Felipe Wolff-Fabris ⁷

¹ Institute of Chemistry and Technology of Macromolecular Materials, Faculty of Chemical Technology, University of Pardubice, 532 10 Pardubice, Czech Republic

² Department of General and Inorganic Chemistry, Faculty of Chemical Technology, University of Pardubice, 532 10 Pardubice, Czech Republic

³ Centre of Polymer Systems, Tomas Bata University in Zlín, 760 01 Zlín, Czech Republic

⁴ Center of Materials and Nanotechnologies, Faculty of Chemical Technology, University of Pardubice, 532 10 Pardubice, Czech Republic

⁵ Institute of Environmental and Chemical Engineering, Faculty of Chemical Technology, University of Pardubice, 532 10 Pardubice, Czech Republic

⁶ Joint Laboratory of Solid State Chemistry, Faculty of Chemical Technology, University of Pardubice, 532 10 Pardubice, Czech Republic

⁷ European Center for Dispersion Technologies, 95100 Selb, Germany

* Correspondence: steinerovadenisa@gmail.com; Tel.: +420-727-843-211

Table S1. Classification scale for the evaluation of coating damage according to CSN ISO 2409.

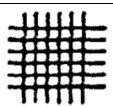
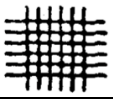
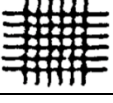
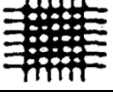

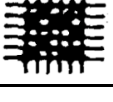
Adhesion evaluation	Appearance	Damage description
0		The edges of the cuts are smooth, no square shows signs of peeling.
1		Slight peeling at intersections of cuts with paint damage up to 5% of the total area.
2		Slight or partial peeling at intersections of cuts with paint damage of 5-15% of the total area.
3		Partial or complete peeling at intersections of sections, or the proportion of sections with paint damage of 15-35% of the total area.
4		Major changes are visible on the paint surface with grid damage ranging from 35-65%.
5		Damage that is greater than 65%.

Table S2. Gardner's iodometric scale.

Degree	1	2	3	4	5	6	7	8	9	10	11	12	13	14
mg I ₂ /100 cm ³	1	2	4	6	10	20	30	45	65	100	150	200	300	500

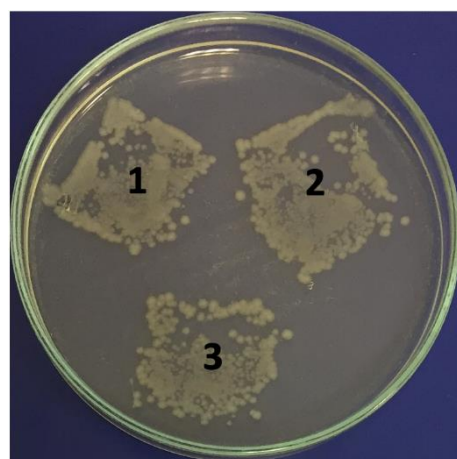
Table S3. Surface roughness determined as RMS (root mean square parameter) of coating films according to ISO 4287.

Sample	RMS (nm)
L ₀	3.2
LMgO-1.5%	3.7
LZnO-1.5%	4.2
LMgO+ZnO-1.75%	2.8
LLa ₂ O ₃ -1.5%	46

Table S4. Statistical ANOVA determination of the effect of concentration and type of nanoparticles on the antimicrobial activity of coatings.

<i>p</i> -value ^a	<i>S. aureus</i>	<i>E. coli</i>	<i>E. faecalis</i>	<i>K. pneumoniae</i>
Concentration ^b	0.000119	0.007467	0.000868	0.003245
Type of nanoparticles ^c	0.098892	0.124811	0.663433	0.105098

^a The threshold value for decision-making is the significance level $\alpha = 0.05$. ^b If the *p*-value is less than 0.05, the effect of the factor is statistically significant. This means that its individual levels will have a different result. This means that the concentration of nanoparticles affects the result of that bacterial test. ^c If the *p*-value is greater than 0.05, the effect of the factor is not statistically significant. This means that at different levels of that factor, the result is statistically the same. This means that the type of nanoparticles used has no effect on bacterial growth.

**Figure S1.** Sorting imprinted on three different agar areas for modified ISO 22196.

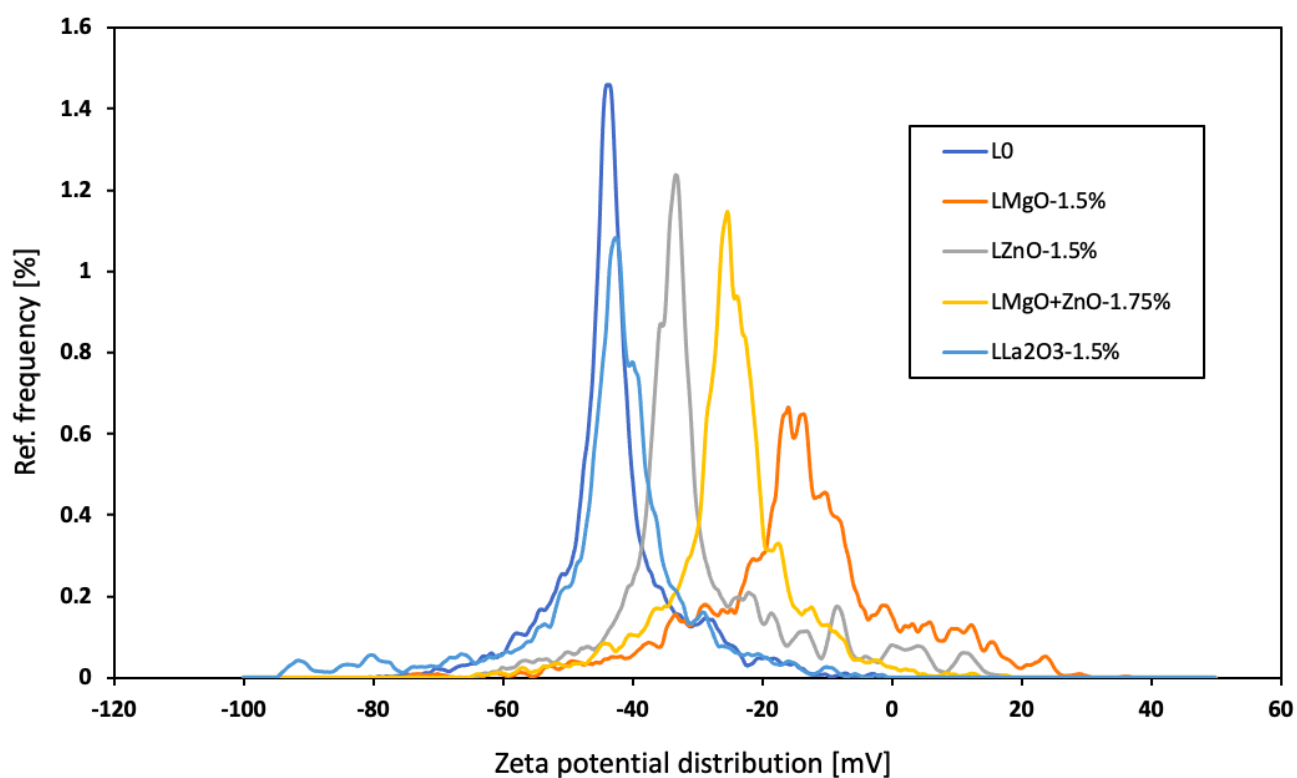


Figure S2. Comparison of zeta potential distribution curves for latexes with the highest concentration of nanoparticles.

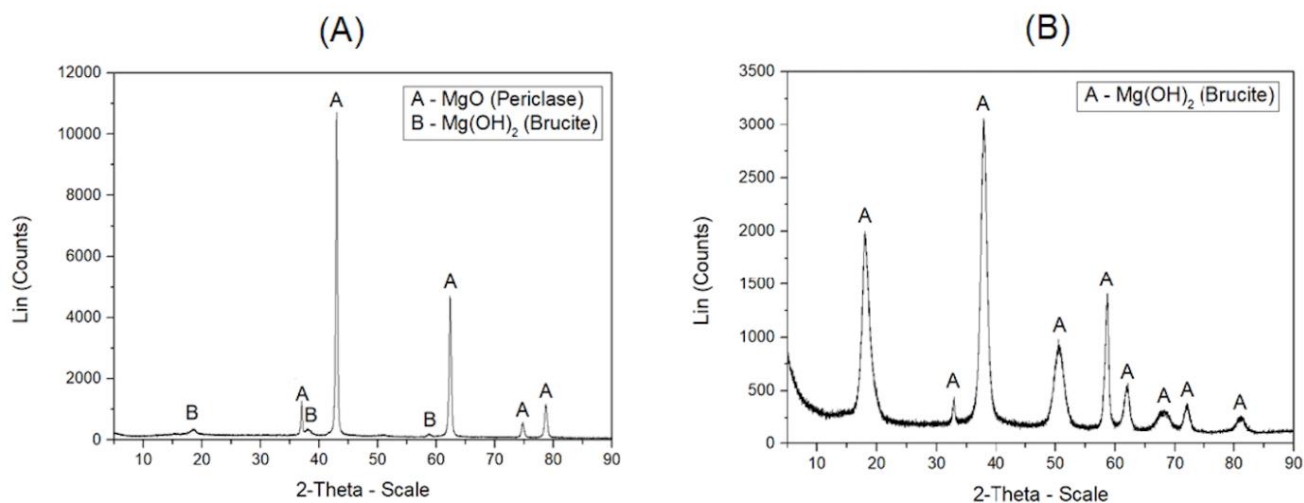


Figure S3. XRD patterns of MgO inorganic nanoparticles: (A) originally supplied; (B) affected by polymerization conditions.

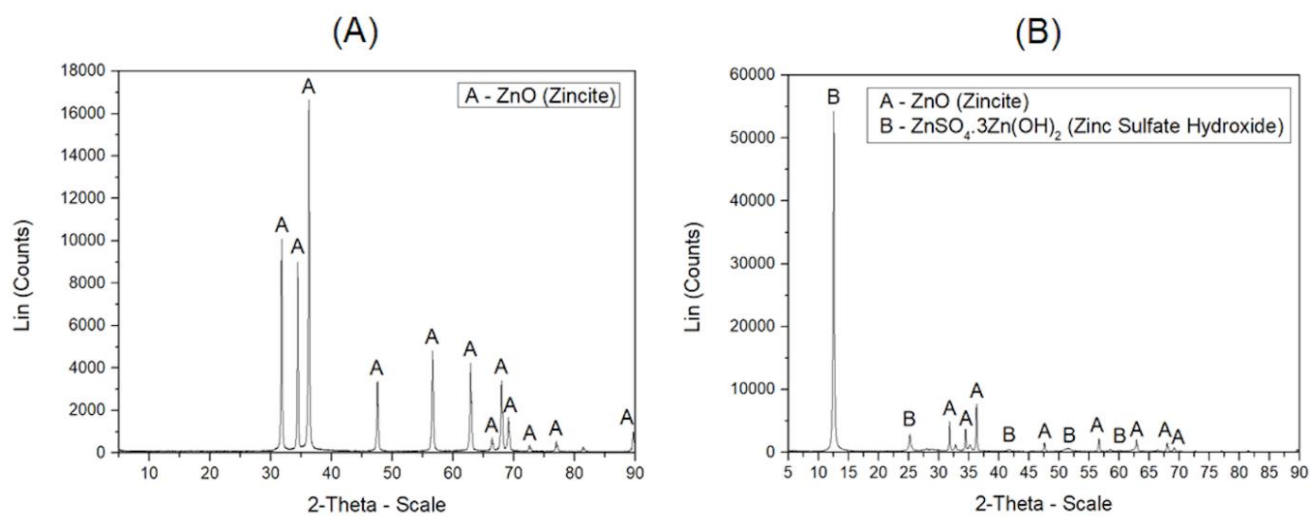


Figure S4. XRD patterns of ZnO inorganic nanoparticles: (A) originally supplied; (B) affected by polymerization conditions.

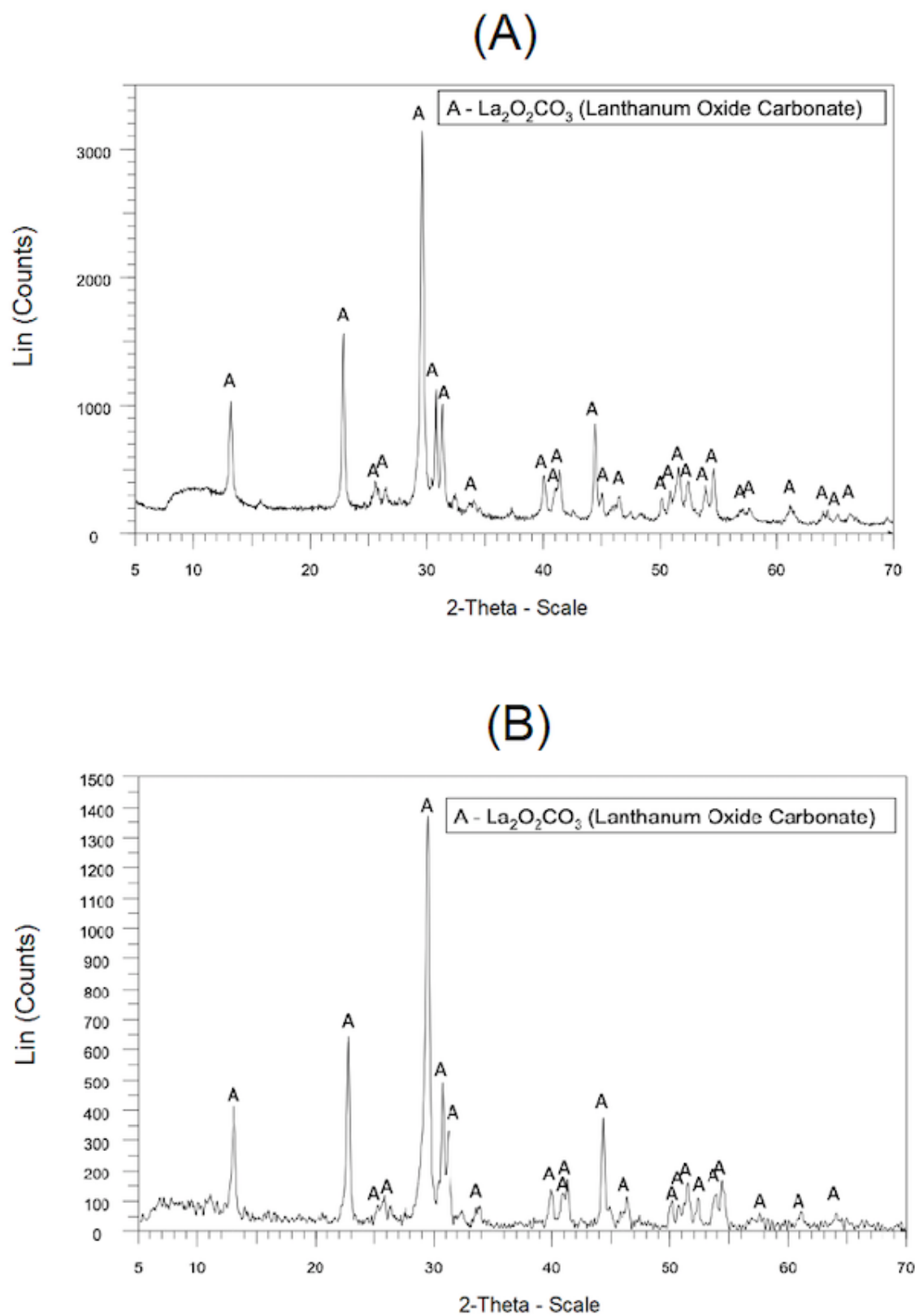


Figure S5. XRD patterns of La_2O_3 inorganic nanoparticles: (A) originally supplied; (B) affected by polymerization conditions.

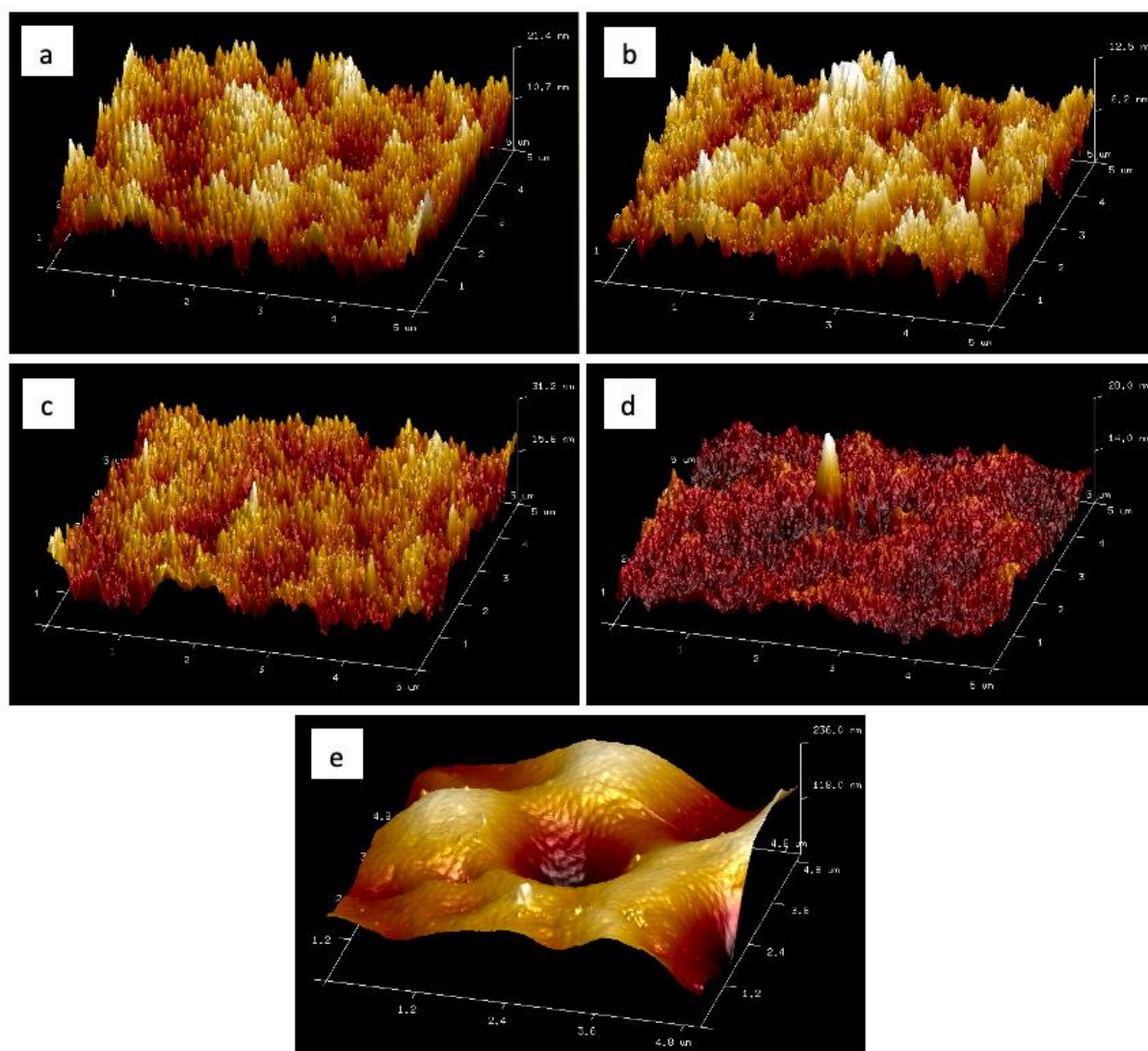


Figure S6. The 3D visualisation of the topographical AFM scans: for blank sample L_0 (a); sample $LMgO-1.5\%$ containing MgO-based nanoparticles (b); sample $LZnO-1.5\%$ containing ZnO-based nanoparticles (c), sample $LMgO+ZnO-1.75\%$ containing MgO-based and ZnO-based nanoparticles (d) and sample $LLa2O3-1.5\%$ containing $La2O3$ -based nanoparticles (e).

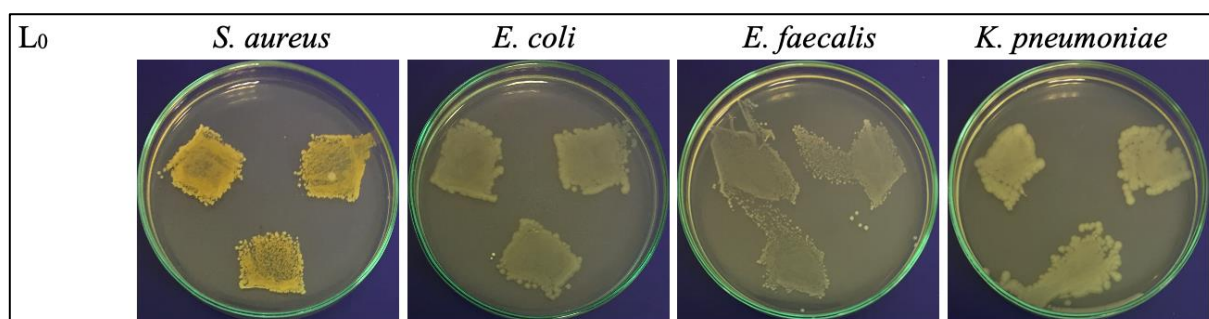


Figure S7. Antimicrobial efficiency of L_0 latex-based coating film according to modified ISO 22196.

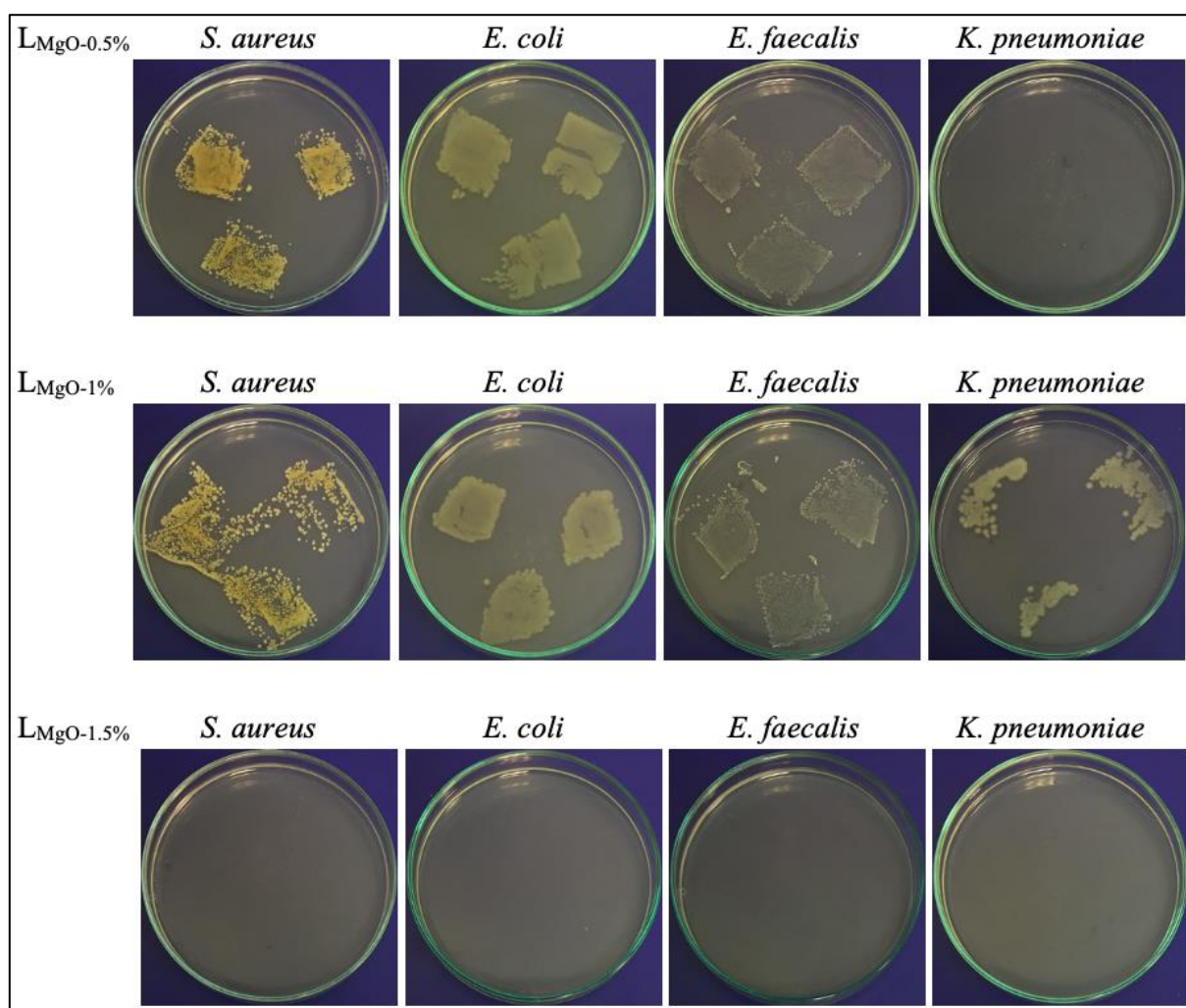


Figure S8. Antimicrobial efficiency of LMgO latex-based coating films according to modified ISO 22196.

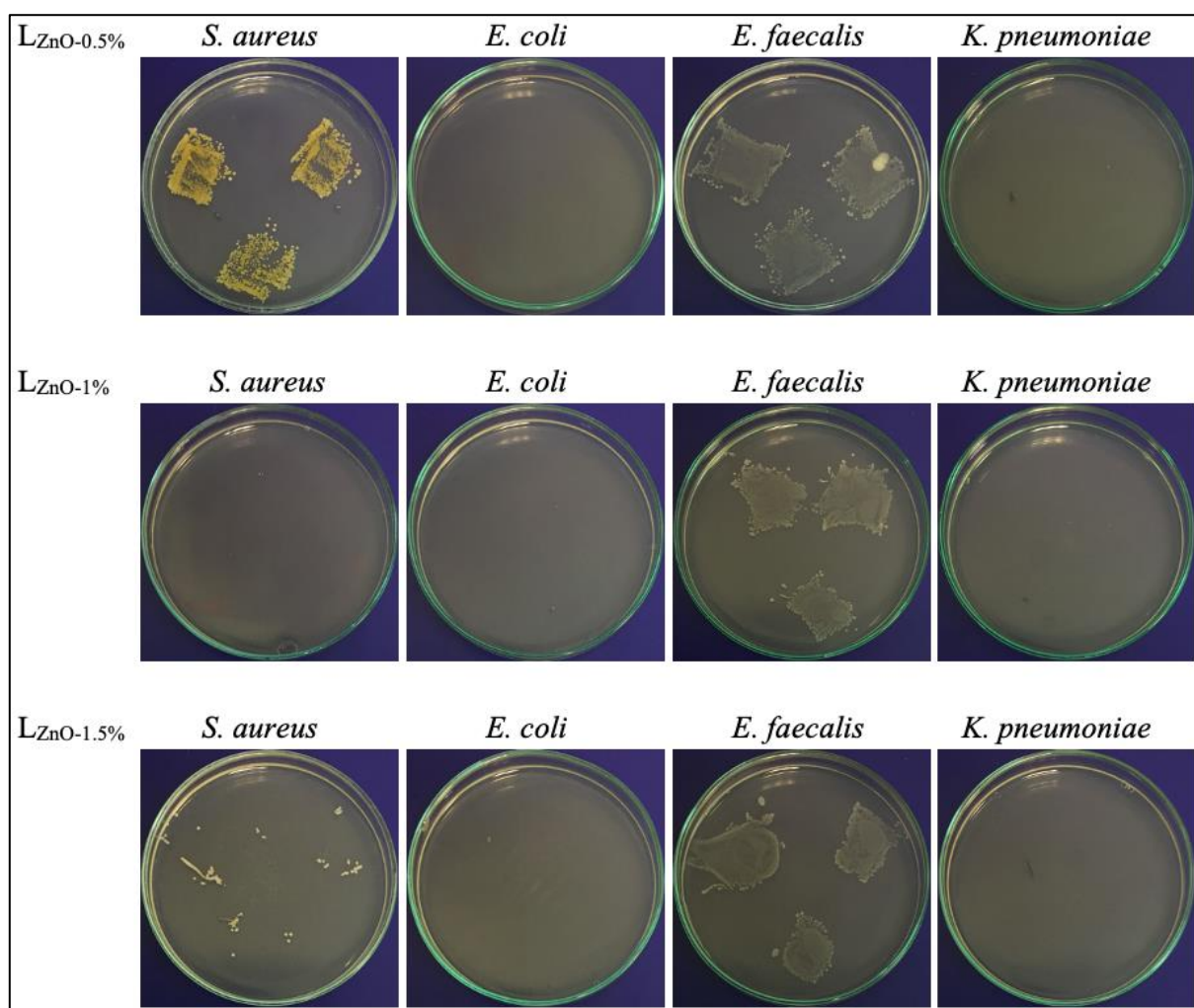


Figure S9. Antimicrobial efficiency of Lzno latex-based coating films according to modified ISO 22196.

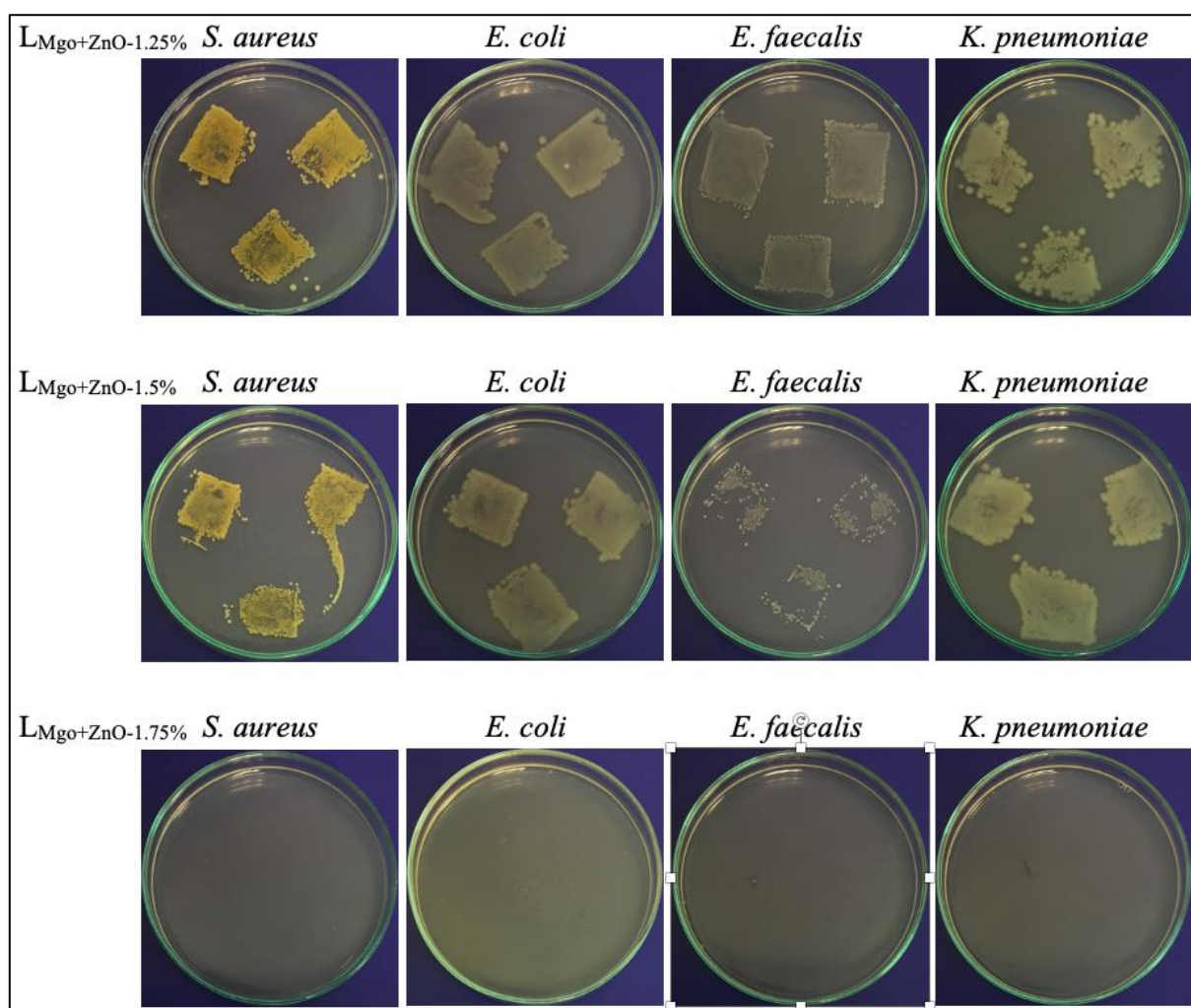


Figure S10. Antimicrobial efficiency of LMgo+ZnO latex-based coating films according to modified ISO 22196.

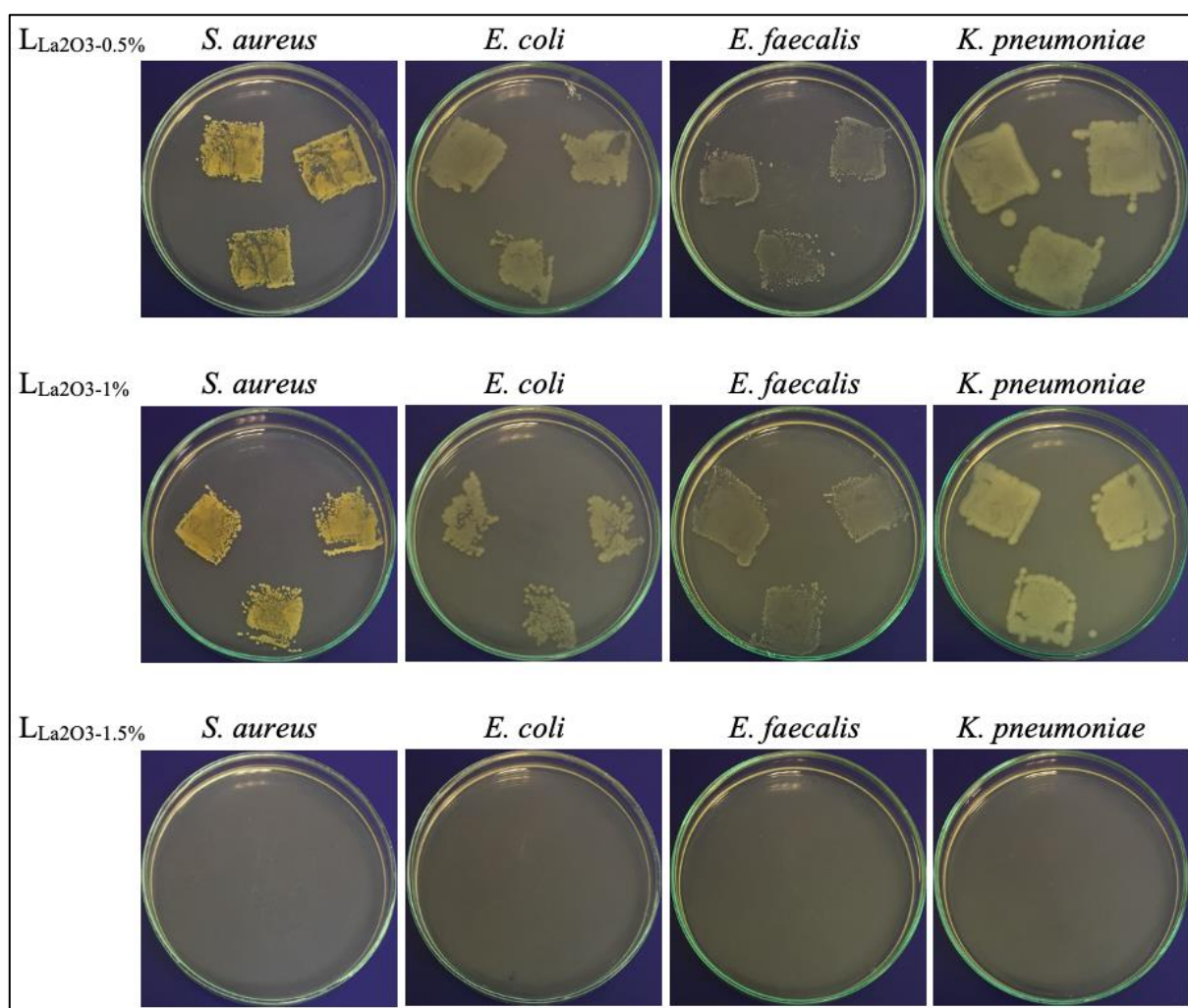


Figure S11. Antimicrobial efficiency of $LLa2O3$ latex-based coating films according to modified ISO 22196.

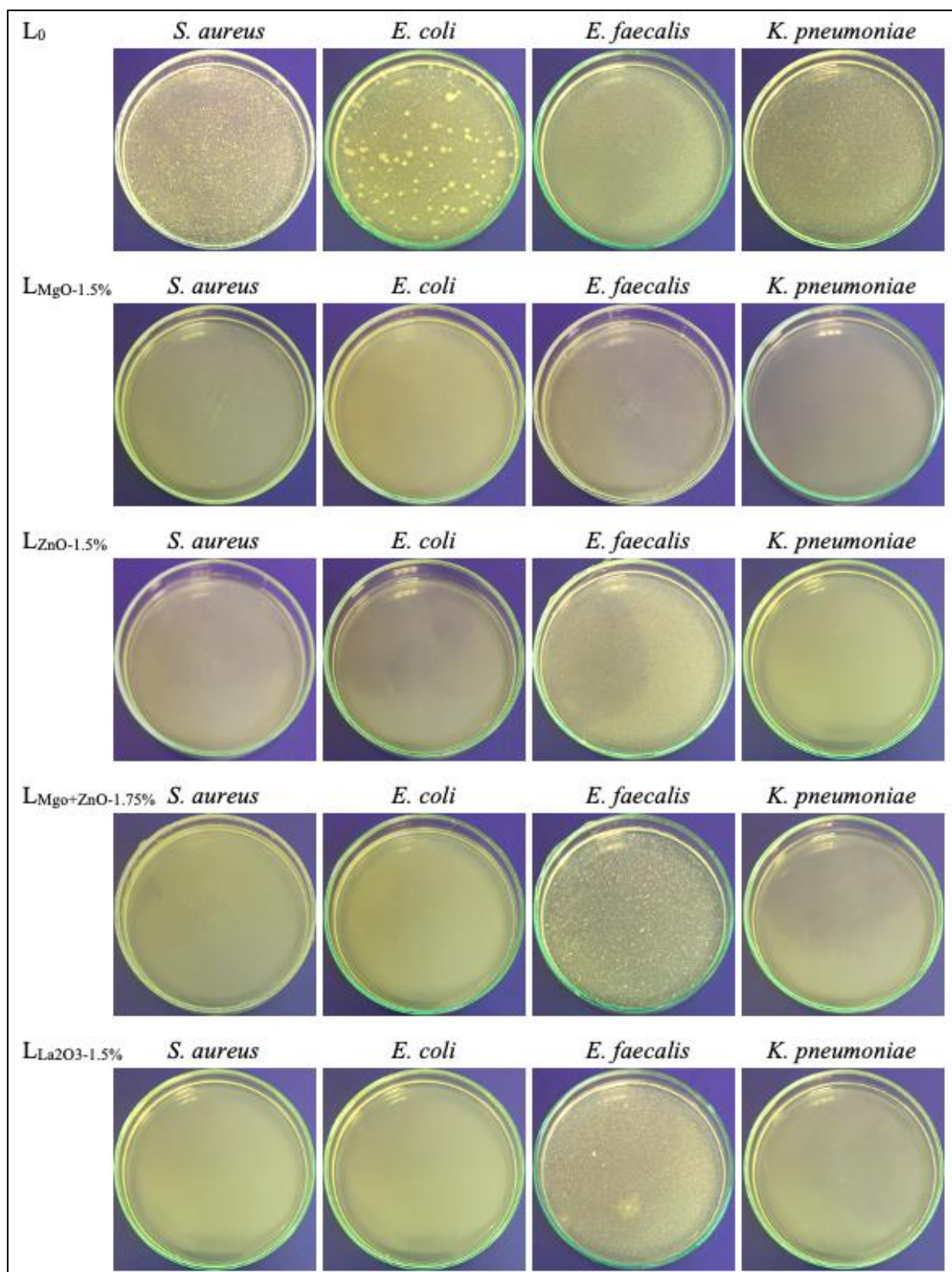


Figure S12. Antimicrobial efficiency of coating films according to ISO 22196.

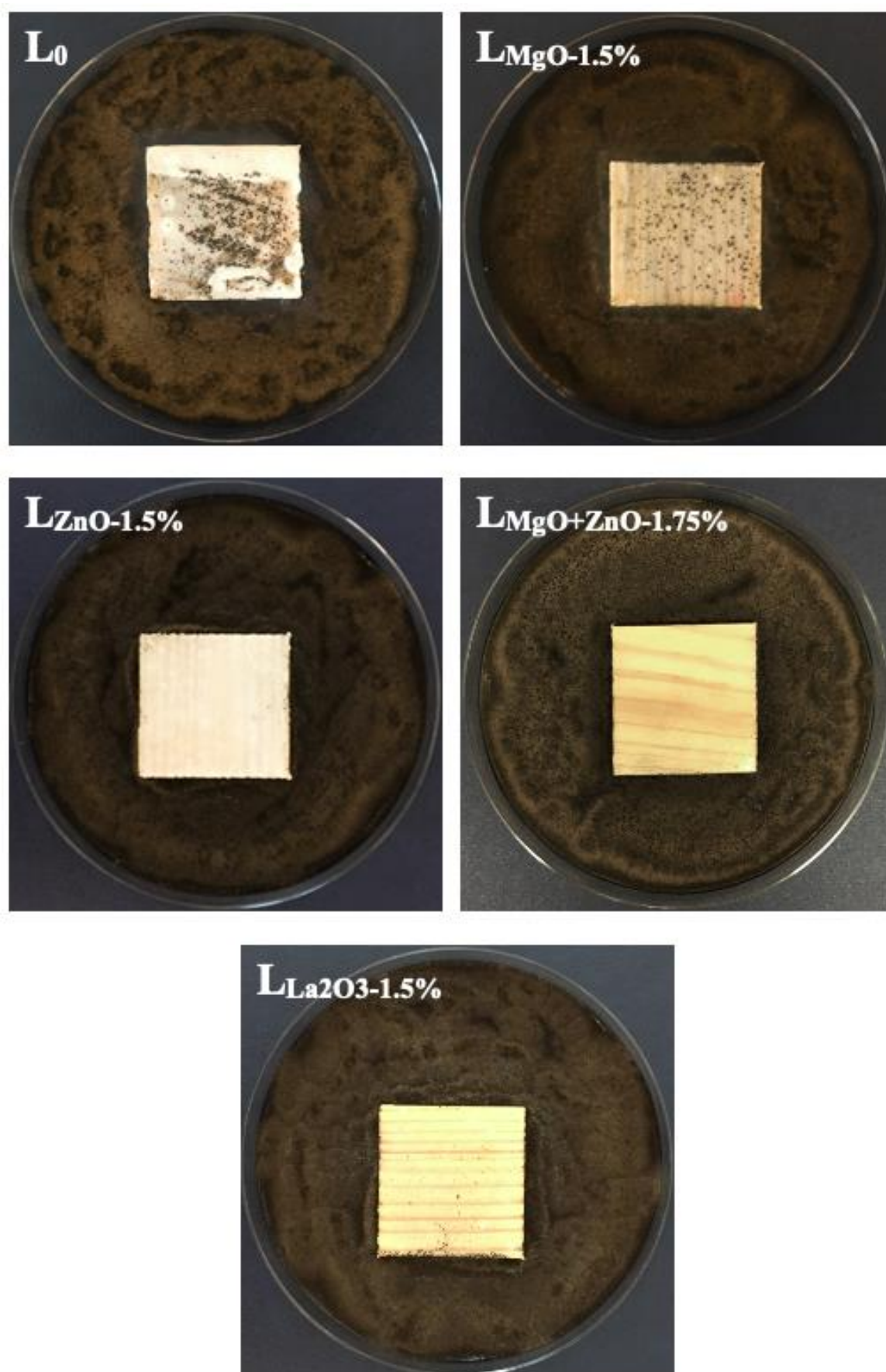


Figure S13. Antifungal efficacy of coating films on wood panels against *A. brasiliensis*.